J. Fluid Mech. (1987), *vol.* 182, *pp.* 447–466
Printed in Great Britain

Shear dispersion looked at from a new angle

By RONALD SMITH

Department of Applied Mathematics and Theoretical Physics, University of Cambridge, Silver Street, Cambridge CB3 9EW, UK

(Received 9 October 1986)

It is shown that for a sudden uniform discharge at $x = 0, t = 0$ in a bounded shear flow, the asymptotic concentration distribution at moderately large times can be well approximated by the tilted Gaussian

$$c = \frac{\overline{q}}{(2\pi\langle\sigma^2\rangle)^{\frac{1}{2}}}\exp\left(-\frac{(x-\overline{u}t-g_0(y,z)+2\alpha D)^2}{2\langle\sigma^2\rangle}\right),$$

with
$$\langle\sigma^2\rangle = 2Dt+2\alpha D(x-\overline{u}t)-3\overline{g_0^2}-4\alpha^2D^2,$$

$$\overline{g_0} = 0, \quad D = \overline{ug_0}, \quad \alpha = \frac{\overline{(u-\overline{u})g_0^2}}{2D^2}.$$

Here $u(y,z)$ is the velocity profile, $g_0(y,z)$ the centroid displacement function, and the overbars denote cross-sectional averaging. The tilt parameter α makes the concentration distribution suitably skew. The effectiveness of this simple formula is demonstrated for two-layer flows and for plane Poiseuille flow.

1. Introduction

The duality between concentration distributions as observed at fixed times or at fixed positions has been the subject of several recent investigations (Tsai & Holley 1978; Chatwin 1980; Smith 1984). The alternative viewpoints share the difficulty that the spatial or temporal concentration distributions are markedly skew. This has the consequence that approximate representations are either inaccurate (e.g. diffusion models) or complicated (e.g. Hermite series with as many as six terms).

Although the asymptotic growth rates of the spatial and temporal variances are proportional to each other (Tsai & Holley 1978, figures 6, 8, 9, 10), the same is not true of the third moments (Tsai & Holley 1978, figures 11, 12). Thus, the question arises whether there is some angle intermediate between the temporal and spatial extremes (i.e. an optimal combination of x and t) for which the corresponding third moment remains bounded. If so, then the comparatively weak and rapidly decaying skewness gives renewed credance to the classical (Taylor 1953; Gill & Sankarasubramanian 1970) use of a Gaussian representation for the longitudinal concentration distribution.

The successful outcome to this quest is stated in §7. The derivation and testing of the approximation is the subject of this paper.

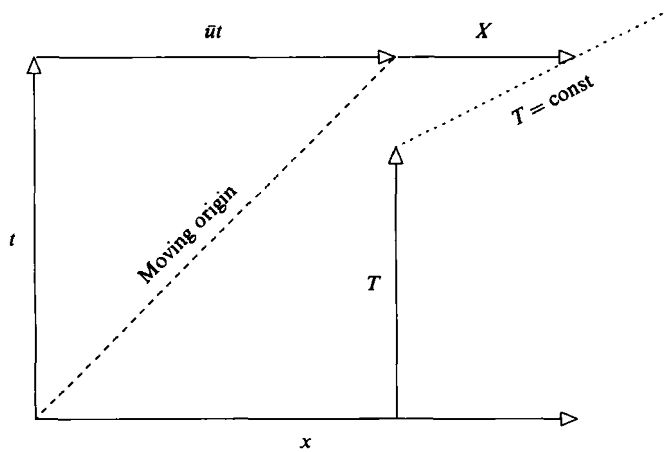

FIGURE 1. Definition sketch showing the geometric relationship between the tilted coordinate system X, T and the conventional coordinates x, t.

2. Tilted and centroid-following coordinate system

For high-Péclet-number plane parallel flow, the advection–diffusion equation takes the form

$$\partial_t c + u\,\partial_x c - \nabla\cdot(\kappa\nabla c) = q, \tag{2.1a}$$

with

$$\kappa \boldsymbol{n}\cdot\nabla c = 0 \quad \text{on } \partial A. \tag{2.1b}$$

Here $u(y,z)$ is the longitudinal velocity, $\kappa(y,z)$ the transverse diffusivity, ∇ the transverse gradient operator $(0, \partial_y, \partial_z)$, $q(x,y,z,t)$ the source strength, ∂A the impermeable boundary, and $\boldsymbol{n}$ its outward normal. The high-Péclet-number assumption means that the longitudinal shear dispersion vastly dominates the direct effects of longitudinal diffusion. Thus, a $\kappa\,\partial_x^2 c$ term has been neglected (Taylor 1953; Aris 1956).

At large times after discharge the contaminant moves along with the bulk velocity $\bar{u}$. Thus, it is convenient to use axes moving with the flow. Also, for reasons explained in §1, we allow a tilt in the orientation of the evolutionary coordinate (see figure 1):

$$T = t + \alpha(x - \bar{u}t), \tag{2.2a}$$

$$X = x - \bar{u}t. \tag{2.2b}$$

The limiting cases $\alpha = 0$, $\alpha\bar{u} = 1$ give predominance respectively to the temporal and spatial evolution of the concentration. The transformation of the field equation (2.1a) is

$$(1 + \alpha u')\,\partial_T c + u'\,\partial_X c - \nabla\cdot(\kappa\nabla c) = q, \tag{2.3a}$$

where

$$u' = u - \bar{u}. \tag{2.3b}$$

The tilt parameter α will be chosen to make a Gaussian approximation for c as accurate as possible.

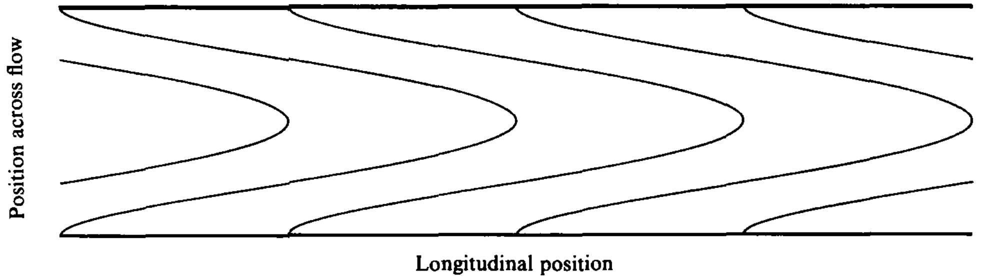

FIGURE 2. Sketch of the centroid-following ξ-coordinate surfaces.

Aris (1956) established that at different levels (y,z) across the flow the centroid is displaced by an amount $g(y,z)$ where

$$\nabla\cdot(\kappa\nabla g) = -u', \tag{2.4a}$$

$$\kappa \boldsymbol{n}\cdot\nabla g = 0 \quad \text{on } \partial A, \tag{2.4b}$$

$$\overline{(1+\alpha u')g} = 0. \tag{2.4c}$$

The overbar denotes a conventional cross-sectional average value. The traditional definition of the centroid displacement function $g_0(y,z)$ corresponds to $\alpha = 0$. The normalization (2.4c) merely gives a shift in value

$$g(y,z) = g_0(y,z) - \alpha\overline{u'g_0}. \tag{2.5}$$

To improve the accuracy of a one-term Gaussian approximation, we shall build the centroid displacement into the coordinate system:

$$\xi = X - g(y,z) = x - \bar{u}t - g(y,z), \tag{2.6}$$

(see figure 2). In the tilted, centroid-following coordinate system the field equation is

$$(1+\alpha u')\,\partial_T c + 2\kappa\nabla g\cdot\nabla\,\partial_\xi c - \kappa(\nabla g)^2\,\partial_\xi^2 c - \nabla\cdot(\kappa\nabla c) = q. \tag{2.7}$$

At first sight (2.7) would appear to be more awkward to study than the original equation (2.1a). However, with the correct choice for α, we find that at large T the solution of (2.7) has a particularly neat form.

3. Moments and weighted means

In the tilted coordinate system we define the moments (Aris 1956; Barton 1983):

$$c^{(j)} = \int_{-\infty}^{\infty} (\xi-\xi_0)^j\, c(\xi,y,z,T)\,\mathrm{d}\xi \quad (j = 0,1,\ldots), \tag{3.1}$$

where the displaced origin ξ_0 will be chosen to make $c^{(1)}$ asymptotically zero. The jth moment of (2.7) gives an equation for $c^{(j)}$:

$$(1+\alpha u')\,\partial_T c^{(j)} - \nabla\cdot(\kappa\nabla c^{(j)}) = q^{(j)} + 2j\kappa\nabla g\cdot\nabla c^{(j-1)} + j(j-1)\,\kappa(\nabla g)^2\, c^{(j-2)}. \tag{3.2}$$

By virtue of the integration with respect to ξ, the $\partial_\xi c$ and $\partial_\xi^2 c$ terms in (2.6) have been replaced by lower-order $c^{(j-1)}$ and $c^{(j-2)}$ forcing terms.

The $(1+\alpha u')$ weighting of the T-derivative in (3.2) leads us to define a weighted average

$$\langle f\rangle = \overline{(1+\alpha u')f}. \tag{3.3}$$

If we make the decomposition

$$c^{(j)} = \langle c^{(j)} \rangle + \delta c^{(j)}, \tag{3.4}$$

then the cross-sectional average of the moment equation (3.2) yields the useful sequels

$$\langle c^{(0)} \rangle = \int_{-\infty}^{T} \overline{q^{(0)}}\, \mathrm{d}T'. \tag{3.5}$$

$$\langle c^{(j)} \rangle = \int_{-\infty}^{T} \overline{q^{(j)}}\, \mathrm{d}T' + 2j \int_{-\infty}^{T} \overline{u'\delta c^{(j-1)}}\, \mathrm{d}T' + j(j-1)\, \overline{\kappa(\nabla g)^2} \int_{-\infty}^{T} \langle c^{(j-2)} \rangle\, \mathrm{d}T' + j(j-1) \int_{-\infty}^{T} \overline{\kappa(\nabla g)^2 \delta c^{(j-2)}}\, \mathrm{d}T'. \tag{3.6}$$

In §§5, 6 it is confirmed that $\delta c^{(0)}$ and $\delta c^{(1)}$ are asymptotically zero. Thus, at $j = 2$ in (3.6) the only persistent forcing stems from $\langle c^{(0)} \rangle$:

$$\langle c^{(2)} \rangle \sim 2\overline{\kappa(\nabla g)^2}\, T \int_{-\infty}^{\infty} \overline{q^{(0)}}\, \mathrm{d}T' + \text{const.} \tag{3.7}$$

The constant depends on the transient behaviour of $q^{(2)}, \delta c^{(0)}, \delta c^{(1)}$ and is the subject of §6. The T-coefficient in (3.7) immediately gives us a formula for the shear dispersion coefficient:

$$D = \overline{\kappa(\nabla g)^2} = \overline{u'g} = \overline{u'g_0} \tag{3.8}$$

(Taylor 1953).

In practice the source strength is given as a function of the original coordinates x, y, z, t. Thus, we note the relationships

$$\int_{-\infty}^{\infty} T^k q^{(j)}\, \mathrm{d}T = \int_{-\infty}^{\infty} \int_{-\infty}^{\infty} (t + \alpha(x - \overline{u}t))^k\, (x - \overline{u}t - \xi_0 - g)^j\, q\, \mathrm{d}x\, \mathrm{d}t. \tag{3.9}$$

In the important limiting case of a sudden discharge at $x = 0, t = 0$ with cross-stream discharge profile $q(y, z)$ we record that

$$\int_{-\infty}^{\infty} q^{(0)}\, \mathrm{d}T' = q(y, z), \tag{3.10a}$$

$$\int_{-\infty}^{\infty} T' q^{(0)}\, \mathrm{d}T' = 0, \tag{3.10b}$$

$$\int_{-\infty}^{\infty} q^{(1)}\, \mathrm{d}T' = -(\xi_0 + g(y, z))\, q(y, z), \tag{3.10c}$$

$$\int_{-\infty}^{\infty} q^{(2)}\, \mathrm{d}T' = (\xi_0 + g(y, z))^2\, q(y, z). \tag{3.10d}$$

For example, at large T, (3.5) yields the asymptote

$$\langle c^{(0)} \rangle \sim \overline{q}. \tag{3.11}$$

4. Choosing the tilt

At $j = 3$ we infer from (3.6) that, since $\langle c^{(1)} \rangle$ and $\delta c^{(1)}$ are asymptotically zero, $\langle c^{(3)} \rangle$ will grow linearly with T unless

$$\overline{u'\delta c^{(2)}} \sim 0 \quad \text{for large } T. \tag{4.1}$$

This is the condition that leads to our selection of the tilt α, i.e. the minimization of the eventual skewness.

From (3.2), (3.5) and (3.7) we deduce that for large T the asymptotic value of $\delta c^{(2)}$ satisfies the equations

$$\nabla\cdot(\kappa\nabla\delta c^{(2)}_{\infty}) = 2\{(1+\alpha u')D-\kappa(\nabla g)^2\}\int_{-\infty}^{\infty}\overline{q^{(0)}}\,\mathrm{d}T, \tag{4.2a}$$

$$\kappa\boldsymbol{n}\cdot\nabla\delta c^{(2)}_{\infty} = 0 \quad \text{on } \partial A, \tag{4.2b}$$

$$\overline{(1+\alpha u')\,\delta c^{(2)}_{\infty}} = 0 \tag{4.2c}$$

By analogy with (2.4*a–c*) for $g(y,z)$ we introduce the excess variance function $R(y,z)$:

$$\nabla\cdot(\kappa\nabla R) = (1+\alpha u')D-\kappa(\nabla g)^2, \tag{4.3a}$$

$$\kappa\boldsymbol{n}\cdot\nabla R = 0 \quad \text{on } \partial A, \tag{4.3b}$$

$$\overline{(1+\alpha u')\,R} = 0, \tag{4.3c}$$

$$R = R_0-\alpha D g_0+\alpha^2D^2-\tfrac{1}{2}\alpha\overline{u'g_0^2}. \tag{4.3d}$$

Thus, we can represent $\delta c^{(2)}_{\infty}$ as

$$\delta c^{(2)}_{\infty} = 2R\int_{-\infty}^{\infty}\overline{q^{(0)}}\,\mathrm{d}T. \tag{4.4}$$

Substituting for $\delta c^{(2)}_{\infty}$ into (4.1), we require that

$$\overline{u'R} = 0. \tag{4.5}$$

From (2.4) and (4.3) satisfied by g and R we can derive the equivalent constraints

$$0 = \overline{u'R} = \overline{\kappa g(\nabla g)^2} = \tfrac{1}{2}\overline{u'g^2}. \tag{4.6}$$

To build the implied value of α into our calculations we modify the definition (2.4*a–c*) of the centroid displacement function $g(y,z)$:

$$\nabla\cdot(\kappa\nabla g) = -u', \tag{4.7a}$$

$$\kappa\boldsymbol{n}\cdot\nabla g = 0 \quad \text{on } \partial A, \tag{4.7b}$$

$$\overline{u'g^2} = 0. \tag{4.7c}$$

The former normalization (2.4*c*) then becomes a definition for α:

$$\alpha = -\frac{\bar{g}}{D} = \frac{\overline{u'g_0^2}}{2D^2}. \tag{4.8}$$

The choice (4.8) ensures that $\langle c^{(3)}\rangle$ remains bounded. Thus, the coefficient of skewness

$$\frac{\langle c^{(3)}\rangle\,\langle c^{(0)}\rangle^{\frac{1}{2}}}{\langle c^{(2)}\rangle^{\frac{3}{2}}} \tag{4.9}$$

decays at the rate $T^{-\frac{3}{2}}$ rather than the usual very slow rate $T^{-\frac{1}{2}}$ (Chatwin 1970, 1980; Nadim, Pagitsas & Brenner 1986).

5. Choosing the displaced origin

At $j = 1$ (3.6) takes the form

$$\langle c^{(1)}\rangle = \int_{-\infty}^{T}\overline{q^{(1)}}\,\mathrm{d}T'+2\int_{-\infty}^{T}\overline{u'\delta c^{(0)}}\,\mathrm{d}T'. \tag{5.1}$$

Before we can eliminate $\langle c^{(1)}\rangle$ at large T, we have to evaluate the $\overline{u'\delta c^{(0)}}$ integral.

From (3.2) and (3.5) we can deduce that the perturbation zero moment $\delta c^{(0)}$ satisfies the field equation

$$(1+\alpha u')\,\partial_T(\delta c^{(0)})-\nabla\cdot(\kappa\nabla\delta c^{(0)}) = q^{(0)}-\overline{q^{(0)}}(1+\alpha u'). \tag{5.2}$$

The forcing term has zero cross-sectional average. Thus, provided that the source is of limited extent and duration, it follows that $\delta c^{(0)}$ tends to zero on a timescale for diffusion across the flow (as was assumed earlier in §3).

Following the pattern of calculations established by Smith (1984, Appendix A), the u' term in the integrand $\overline{u'\delta c^{(0)}}$ leads us to consider (4.7*a–c*) satisfied by the centroid displacement function $g(y,z)$. The two field equations (4.7*a*) and (5.2) satisfied by g and $\delta c^{(0)}$ can be combined:

$$\partial_T\{g(1+\alpha u')\,\delta c^{(0)}\}-\nabla\cdot(g\kappa\nabla\delta c^{(0)})+\nabla\cdot(\delta c^{(0)}\kappa\nabla g) = g(q^{(0)}-\overline{q^{(0)}}(1+\alpha u'))-u'\delta c^{(0)}. \tag{5.3}$$

Integrating this composite equation across the flow and with respect to T, we arrive at the result

$$\int_{-\infty}^{T}\overline{u'\delta c^{(0)}}\,\mathrm{d}T' = \int_{-\infty}^{T}\overline{gq^{(0)}}\,\mathrm{d}T'-\overline{g(1+\alpha u')\,\delta c^{(0)}}. \tag{5.4}$$

The transience of $\delta c^{(0)}$ ensures that the final term vanishes for large T.

Returning to (5.1) we have the asymptote

$$\langle c^{(1)}\rangle \sim \int_{-\infty}^{\infty}\overline{q^{(1)}}\,\mathrm{d}T'+2\int_{-\infty}^{\infty}\overline{gq^{(0)}}\,\mathrm{d}T'. \tag{5.5}$$

For the special case of a sudden discharge at $x=0, t=0$ we use (3.10*a, c*) to obtain

$$\langle c^{(1)}\rangle \sim -\xi_0\bar{q}+\overline{gq}. \tag{5.6}$$

Hence we choose the displaced origin

$$\xi_0 = \frac{\overline{gq}}{\bar{q}}. \tag{5.7}$$

The field equation (2.4*a*) or (4.7*a*) satisfied by $g(x,y)$ suggests that the g-profile closely follows the u' profile. Hence, a discharge where the flow is fast can be expected to be displaced forwards. Less obviously, there is dependence upon α:

$$\xi_0 = \frac{\overline{g_0 q}}{\bar{q}}-\alpha D, \tag{5.8a}$$

$$X_0 = \xi_0+g_0-\alpha D = \frac{\overline{g_0 q}}{\bar{q}}+g_0-2\alpha D. \tag{5.8b}$$

The difference between the values of the centroid position X_0 in the cases $\alpha=0, \alpha\bar{u}=1$ has been remarked upon by Tsai & Holley (1978) and by Smith (1984, equations (11.1), (11.4)). At a fixed position, contaminant that arrives later has had more time to be dispersed. This extra spreading gives a shift of the centroid towards later times, i.e. to negative X.

6. Asymptotic second moment

When written in full (3.7) becomes

$$\langle c^{(2)}\rangle \approx 2DT\int_{-\infty}^{\infty}\overline{q^{(0)}}\,\mathrm{d}T'-2D\int_{-\infty}^{\infty}T'\overline{q^{(0)}}\,\mathrm{d}T'+\int_{-\infty}^{\infty}\overline{q^{(2)}}\,\mathrm{d}T' +4\int_{-\infty}^{\infty}\overline{u'\delta c^{(1)}}\,\mathrm{d}T'+2\int_{-\infty}^{\infty}\overline{\kappa(\nabla g)^2\,\delta c^{(0)}}\,\mathrm{d}T'. \quad (6.1)$$

Thus, we have to contend with integrals involving $\delta c^{(1)}$ and $\delta c^{(0)}$.

The field equation for the perturbation first moment $\delta c^{(1)}$ can be written

$$(1+\alpha u')\,\partial_T(\delta c^{(1)})-\nabla\cdot(\kappa\nabla\delta c^{(1)}) = q^{(1)}-(1+\alpha u')\,\overline{q^{(1)}}+2(u'\delta c^{(0)}-(1+\alpha u')\,\overline{u\delta c^{(0)}})+2\nabla\cdot(\delta c^{(0)}\kappa\nabla g). \quad (6.2)$$

As was the case with (5.2) for $\delta c^{(0)}$, there is no net discharge, and the right-hand-side forcing terms are all transient. Hence (as was assumed in §3), $\delta c^{(1)}$ tends to zero on the timescale for diffusion across the flow. Of course, all this means is that at large times the use of centroid-following coordinates has achieved the stated objective of accurately following the centroid and of eliminating $\delta c^{(1)}$.

To evaluate the $\overline{u\delta c^{(1)}}$ integral we commence with a composite equation satisfied by g and $\delta c^{(1)}$:

$$\partial_T\{g(1+\alpha u')\,\delta c^{(1)}\}-\nabla\cdot(g\kappa\nabla\delta c^{(1)})+\nabla\cdot(\delta c^{(1)}\kappa\nabla g) = -u'\delta c^{(1)}+g(q^{(1)}-\overline{q^{(1)}}(1+\alpha u'))-2g(1+\alpha u')\,\overline{u'\delta c^{(0)}} +2\nabla\cdot(\kappa g\delta c^{(0)}\nabla g)+2\delta c^{(0)}(u'g-\kappa(\nabla g)^2). \quad (6.3)$$

Integrating across the flow and with respect to T we obtain

$$\int_{-\infty}^{T}\overline{u'\delta c^{(1)}}\,\mathrm{d}T' = \int_{-\infty}^{T}\overline{gq^{(1)}}\,\mathrm{d}T'+2\int_{-\infty}^{T}\overline{(u'g-\kappa(\nabla g)^2)\,\delta c^{(0)}}\,\mathrm{d}T'-\overline{g(1+\alpha u')\,\delta c^{(1)}}. \quad (6.4)$$

Hence, in (6.1) the $\overline{u'\delta c^{(1)}}$ integral can be replaced by integrals involving $\delta c^{(0)}$.

To evaluate the $\overline{\kappa(\nabla g)^2\,\delta c^{(0)}}$ integral we construct a composite equation satisfied by $R(y,z)$ and $\delta c^{(0)}$:

$$\partial_T\{R(1+\alpha u')\,\delta c^{(0)}\}-\nabla\cdot(R\kappa\nabla\delta c^{(0)})+\nabla\cdot(\delta c^{(0)}\kappa\nabla R) = R(q^{(0)}-\overline{q^{(0)}}(1+\alpha u'))+(1+\alpha u')\,D\delta c^{(0)}-\kappa(\nabla g)^2\,\delta c^{(0)}. \quad (6.5)$$

Integrating across the flow and with respect to T, we derive the asymptote

$$\int_{-\infty}^{\infty}\overline{\kappa(\nabla g)^2\,\delta c^{(0)}}\,\mathrm{d}T' \sim \int_{-\infty}^{\infty}\overline{Rq^{(0)}}\,\mathrm{d}T'. \quad (6.6)$$

For the $\overline{u'g\delta c^{(0)}}$ integral, we first introduce the auxiliary function $g^{(2)}(y,z)$:

$$\nabla\cdot(\kappa\nabla g^{(2)}) = (1+\alpha u')\,D-ug, \quad (6.7a)$$

$$\kappa\boldsymbol{n}\cdot\nabla g^{(2)} = 0 \quad \text{on } \partial A. \quad (6.7b)$$

$$\overline{(1+\alpha u')\,g^{(2)}} = 0, \quad (6.7c)$$

with

$$g^{(2)} = R+\tfrac{1}{2}g^2-\tfrac{1}{2}\overline{(1+\alpha u')\,g^2}. \quad (6.7d)$$

The composite equation satisfied by $g^{(2)}$ and $\delta c^{(0)}$ is

$$\partial_T\{g^{(2)}(1+\alpha u')\,\delta c^{(0)}\} - \nabla\cdot(g^{(2)}\kappa\nabla\delta c^{(0)}) + \nabla\cdot(\delta c^{(0)}\kappa\nabla g) = g^{(2)}(q^{(0)} - \overline{q^{(0)}}(1+\alpha u')) + (1+\alpha u')\,D\delta c^{(0)} - ug\delta c^{(0)}. \quad (6.8)$$

In the now familiar manner, we integrate across the flow and with respect to T, deriving the asymptote

$$\int_{-\infty}^{\infty} \overline{u'g\delta c^{(0)}}\,\mathrm{d}T' \sim \int_{-\infty}^{\infty} \overline{g^{(2)}q^{(0)}}\,\mathrm{d}T'. \quad (6.9)$$

The expressions (5.4), (6.6) and (6.9) for the various $\delta c^{(0)}$ integrals permit us to evaluate the asymptotic expression for $\langle c^{(2)}\rangle$:

$$\langle c^{(2)}\rangle \sim 2DT\int_{-\infty}^{\infty}\overline{q^{(0)}}\,\mathrm{d}T' - 2D\int_{-\infty}^{\infty} T'\overline{q^{(0)}}\,\mathrm{d}T' + \int_{-\infty}^{\infty}\overline{q^{(2)}}\,\mathrm{d}T' + 4\int_{-\infty}^{\infty}\overline{gq^{(1)}}\,\mathrm{d}T' + 8\int_{-\infty}^{\infty}\overline{g^{(2)}q^{(0)}}\,\mathrm{d}T' - 6\int_{-\infty}^{\infty}\overline{Rq^{(0)}}\,\mathrm{d}T'. \quad (6.10)$$

For the special case of a sudden discharge at $x=0, t=0$ with ξ_0 given by (5.7), this simplifies to

$$\langle c^{(2)}\rangle \sim 2TD\overline{q} - \frac{(\overline{gq})^2}{\overline{q}} - 3\overline{g^2q} + 8\overline{g^{(2)}q} - 6\overline{Rq}. \quad (6.11)$$

If we eliminate $g^{(2)}$ in favour of R, by means of (6.7d), then the asymptotic second moment can be expressed

$$\frac{\langle c^{(2)}\rangle}{\langle c^{(0)}\rangle} \sim 2DT - 4\overline{(1+\alpha u')g^2} + \frac{\overline{g^2q}}{\overline{q}} - \left(\frac{\overline{gq}}{\overline{q}}\right)^2 + 2\frac{\overline{Rq}}{\overline{q}}. \quad (6.12)$$

To include the (y,z)-dependence of $c^{(2)}$, we need to add together the asymptotic results (6.12) and (4.4) for $\langle c^{(2)}\rangle$ and for $\delta c^{(2)}_{\infty}$:

$$\sigma^2 = \frac{c^{(2)}}{c^{(0)}} \sim 2DT - 4\overline{g^2} - 4\alpha\overline{u'g^2} + \frac{\overline{g^2q}}{\overline{q}} - \left(\frac{\overline{gq}}{\overline{q}}\right)^2 + 2\frac{\overline{Rq}}{\overline{q}} + 2R(y,z). \quad (6.13)$$

To explicitly reveal the α-dependence we use (2.5) and (4.3d) to replace g and R in terms of g_0 and R_0:

$$\sigma^2 = \frac{c^{(2)}}{c^{(0)}} \sim 2DT - 4\overline{g_0^2} + \frac{\overline{g_0^2q}}{\overline{q}} - \left(\frac{\overline{g_0q}}{\overline{q}}\right)^2 + 2\frac{\overline{R_0q}}{\overline{q}} + 2R_0 - 2\alpha D\left(\frac{\overline{g_0q}}{\overline{q}} + g_0\right) - 6\alpha\overline{u'g_0^2} + 8\alpha^2D^2. \quad (6.14)$$

For the special cases $\alpha = 0, \alpha\overline{u} = 1$ this equation agrees with Smith (1984, equations (11.8), (11.9)). Remarkably, Tsai & Holley (1980) were able to identify the 6α-coefficient from their numerical work.

For uniform discharges and with the optimal choice for α, (6.13) becomes

$$\sigma^2 \sim 2DT - 3\overline{g^2} - \alpha^2D^2 + 2R(y,z), \quad (6.15a)$$

$$\langle\sigma^2\rangle \sim 2DT - 3\overline{g^2} - \alpha^2D^2 = 2DT - 3\overline{g_0^2} - 4\alpha^2D^2. \quad (6.15b)$$

7. Gaussian approximations

Nadim *et al.* (1986) warn of the inconsistencies, such as negative concentrations, that can arise beyond a Gaussian approximation. Yet, as expounded by Chatwin (1970, 1980), the usefulness of a Gaussian approximation to the longitudinal concentration distribution is severely limited by the slow decay (as $t^{-\frac{1}{2}}$) of the skewness. What has been achieved here by the use of tilted, centroid-following coordinates

$$T = t+\alpha(x-\overline{u}t), \tag{7.1a}$$

$$\xi = x-\overline{u}t-g(y,z) \tag{7.1b}$$

$$\alpha = \frac{-\overline{g}}{D} \tag{7.1c}$$

is an accelerated decay (as $T^{-\frac{3}{2}}$) of the skewness. The centroid-displacement function $g(y,z)$ is defined by the cross-stream equations

$$\nabla\cdot(\kappa\nabla g) = \overline{u}-u, \tag{7.2a}$$

$$\kappa \boldsymbol{n}\cdot\nabla g = 0 \quad \text{on } \partial A, \tag{7.2b}$$

$$\overline{(u-\overline{u})\,g^2} = 0, \tag{7.2c}$$

with

$$D = \overline{\kappa(\nabla g)^2} = \overline{(u-\overline{u})\,g}. \tag{7.2d}$$

For a sudden discharge at $x = 0, t = 0$ with cross-stream profile $q(y,z)$ the asymptotic zero moment, centroid and variance are

$$c^{(0)} = \overline{q}, \tag{7.3a}$$

$$\xi_0 = \frac{\overline{gq}}{\overline{q}}, \tag{7.3b}$$

$$\sigma^2 = 2DT-4\overline{g^2}+\frac{\overline{g^2q}}{\overline{q}}-\left(\frac{\overline{gq}}{\overline{q}}\right)^2+2\frac{\overline{Rq}}{\overline{q}}+2R(y,z). \tag{7.3c}$$

Here the excess variance function $R(y,z)$ satisfies the cross-stream equations

$$\nabla\cdot(\kappa\nabla R) = (1+\alpha(u-\overline{u}))\,D-\kappa(\nabla g)^2, \tag{7.4a}$$

$$\kappa\boldsymbol{n}\cdot\nabla R = 0 \quad \text{on } \partial A, \tag{7.4b}$$

$$\overline{R} = 0. \tag{7.4c}$$

A Gaussian approximation that reproduces the asymptotes (7.3*a*–*c*) is

$$c = \frac{\overline{q}}{\sigma(2\pi)^{\frac{1}{2}}}\exp\left[-\frac{1}{2}\left(\frac{\xi-\xi_0}{\sigma}\right)^2\right]. \tag{7.5}$$

Since our calculations have only extended as far as the third moment, it follows that the dominant error is associated with the fourth moment. From the work of Chatwin (1970, 1980) we can infer that for large T the relative error decays at the modest rate T^{-1}.

For uniform discharges it is tempting to avoid the calculation of the excess variance function $R(y,z)$. First, we note that the $\overline{Rq}$ contribution to the variance is zero. Next, if we write

$$\sigma^2 = \langle\sigma^2\rangle+2R(y,z), \tag{7.6}$$

then (7.5) can be expanded in powers of $R/\langle\sigma^2\rangle$:

$$c = \frac{\bar{q}}{(2\pi\langle\sigma^2\rangle)^{\frac{1}{2}}}\exp(-\tfrac{1}{2}\zeta^2)\left\{1+\frac{R(y,z)}{\langle\sigma^2\rangle}\mathrm{He}_2(\zeta)+\frac{1}{2}\left(\frac{R}{\langle\sigma^2\rangle}\right)^2\mathrm{He}_4(\zeta)+\ldots\right\}, \quad (7.7a)$$

where

$$\zeta = \frac{\xi-\xi_0}{\langle\sigma^2\rangle^{\frac{1}{2}}}, \quad (7.7b)$$

$$\mathrm{He}_2(\zeta) = \zeta^2-1, \quad \mathrm{He}_4(\zeta) = \zeta^4-6\zeta^2+6. \quad (7.7c, d)$$

The selection (7.1 c) of α ensures that the two averages $\overline{R}$ and $\langle R\rangle$ are both zero. Hence we can expect the function $R(y,z)$ to be relatively small (as compared say to g^2). This leads to the Gaussian approximation

$$c = \frac{\bar{q}}{(2\pi\langle\sigma^2\rangle)^{\frac{1}{2}}}\exp\left(-\frac{(x-\bar{u}t-g(y,z)+\alpha D)^2}{2\langle\sigma^2\rangle}\right) \quad (7.8a)$$

with

$$\langle\sigma^2\rangle = 2Dt+2\alpha D(x-\bar{u}t)-3\overline{g^2}-\alpha^2D^2. \quad (7.8b)$$

In terms of g_0 this can be rewritten as

$$c = \frac{\bar{q}}{(2\pi\langle\sigma^2\rangle)^{\frac{1}{2}}}\exp\left(-\frac{(x-\bar{u}t-g_0(y,z)+2\alpha D)^2}{2\langle\sigma^2\rangle}\right), \quad (7.9a)$$

with

$$\langle\sigma^2\rangle = 2Dt+2\alpha D(x-\bar{u}t)-3\overline{g_0^2}-4\alpha^2D^2. \quad (7.9b)$$

Sometimes it is only the cross-sectionally averaged concentration $\bar{c}$ that is required. If we define

$$\Sigma^2 = 2Dt+2\alpha D(x-\bar{u}t)-2\overline{g_0^2}-4\alpha^2D^2, \quad (7.10)$$

then (7.8a) can be expanded:

$$c = \frac{\bar{q}}{(2\pi\Sigma^2)^{\frac{1}{2}}}\exp(-\tfrac{1}{2}\zeta^2)\left\{1-\frac{g_0(y,z)}{\Sigma}\mathrm{He}_1(\zeta)+\frac{g_0^2-\overline{g_0^2}}{\Sigma^2}\mathrm{He}_2(\zeta)\right.$$

$$\left.+\frac{g_0^3}{6\Sigma^3}\mathrm{He}_3(\zeta)+\frac{g_0^4+12(\overline{g_0^2})^2}{24\Sigma^4}\mathrm{He}_4(\zeta)+\ldots\right\}, \quad (7.11a)$$

where

$$\zeta = \frac{x-\bar{u}t+2\alpha D}{\Sigma}, \quad (7.11b)$$

$$\mathrm{He}_1(\zeta) = \zeta, \quad \mathrm{He}_3(\zeta) = \zeta^3-3\zeta. \quad (7.11c, d)$$

By definition $g_0(y,z)$ has zero cross-sectional average. Also, the particular choice (7.10) for Σ^2 is designed to ensure that the $\mathrm{He}_2(\zeta)$ coefficient has a zero cross-sectional average. Thus, for $\bar{c}(x,t)$ we pose the Gaussian approximation

$$\bar{c} = \frac{\bar{q}}{(2\pi\Sigma^2)^{\frac{1}{2}}}\exp\left(\frac{(x-\bar{u}t+2\alpha D)^2}{2\Sigma^2}\right). \quad (7.12)$$

At large times the area, centroid, variance and growth rate of the third moment are all asymptotically correct. It is this final ingredient, associated with the tilt parameter α, that makes the tilted Gaussian an improvement upon conventional Gaussian representations.

8. Two-layer flows

The exact solution given by Thacker (1976) for two-layer flows provides a convenient means of testing the accuracy of the asymptotic solution (7.5). We denote the layer velocities by u_+, u_- and the e-folding rate for mixing between the two layers by λ. The advection–diffusion equation (2.1 a) is replaced by the pair of equations

$$\partial_t c_+ + u_+ \partial_x c_+ = \lambda a_-(c_- - c_+) + q_+, \tag{8.1a}$$

$$\partial_t c_- + u_- \partial_x c_- = \lambda a_+(c_+ - c_-) + q_-. \tag{8.1b}$$

Here c_+, c_- are the concentrations in each of the well-mixed layers, q_+, q_- are the source strengths within each layer, and a_+, a_- are the fractional areas of the layers:

$$a_+ = \frac{\overline{u} - u_-}{u_+ - u_-}, \quad a_- = \frac{u_+ - \overline{u}}{u_+ - u_-}. \tag{8.2a, b}$$

If we choose to eliminate c_-, then we find that c_+ satisfies a telegraph equation

$$\partial_t c_+ + \overline{u}\,\partial_x c_+ + \frac{1}{\lambda}(\partial_t + u_- \partial_x)(\partial_t + u_+ \partial_x) c_+ = a_- q_- + \frac{1}{\lambda}(\partial_t + u_- \partial_x + a_+ \lambda) q_+. \tag{8.3}$$

For a sudden discharge at $x = 0, t = 0$ the upper-layer concentration c_+ has a modified-Bessel-function representation confined to the range $u_- t < x < u_+ t$:

$$c_+ = \frac{\lambda}{u_+ - u_-}\left(q_- a_- I_0(r) + 2q_+ \frac{a_+ a_- \lambda(x - u_- t)}{(u_+ - u_-) r} I_1(r)\right) \times \exp\left(-\lambda \frac{(a_-(x - u_- t) + a_+(u_+ t - x))}{u_+ - u_-}\right), \tag{8.4a}$$

with

$$r^2 = 4\lambda^2 a_+ a_- \frac{(x - u_- t)(u_+ t - x)}{(u_+ - u_-)^2}, \tag{8.4b}$$

together with a decaying delta-function singularity moving at the layer velocity:

$$c_+ = q_+ \delta(x - u_+ t) \exp(-a_- \lambda t). \tag{8.4c}$$

The inclusion of longitudinal diffusion within each layer removes these spikes, but the corresponding analytic solution is much more complicated (Chickwendu & Ojiakor 1985).

To apply the analysis of the present paper, we first need to evaluate the centroid displacement function g:

$$g_+ = \frac{u_+ - u_-}{2\lambda}, \quad g_- = -\frac{(u_+ - u_-)}{2\lambda}. \tag{8.5a, b}$$

From g_+, g_- we can evaluate the shear dispersion coefficient and the tilt parameter:

$$D = a_+ a_- \frac{(u_+ - u_-)^2}{\lambda} = \frac{(u_+ - \overline{u})(\overline{u} - u_-)}{\lambda}, \tag{8.6a}$$

$$\alpha = -\frac{(a_+ - a_-)}{2a_+ a_-}\frac{1}{(u_+ - u_-)} = \frac{(u_+ + u_-) - 2\overline{u}}{2(u_+ - \overline{u})(\overline{u} - u_-)}. \tag{8.6b}$$

Conveniently, the two properties $\overline{R} = 0, \langle R \rangle = 0$ of the excess variance function ensure that

$$R_+ = R_- = 0. \tag{8.7}$$

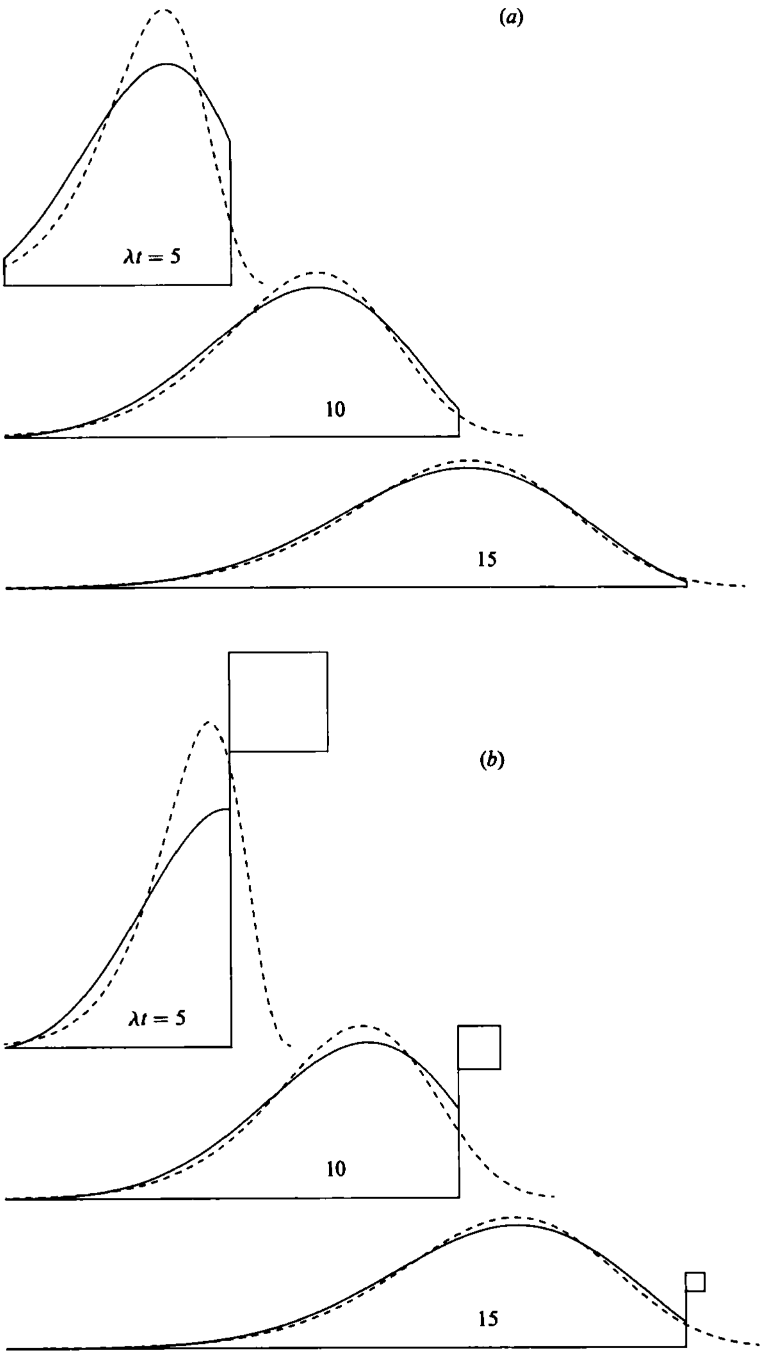

Figure 3. Comparison between the exact (——) and tilted Gaussian (----) concentration distributions at times $\lambda t = 5, 10, 15$ for the upper-layer concentration with (*a*) a lower-layer discharge in a two-layer flow, and (*b*) an upper-layer discharge in a two-layer flow. The area under the delta-function spikes is indicated by the area of the flags.

Thus (7.3*b*, *c*) for the centroid displacement ξ_0 and the variance σ^2 take the form

$$\xi_0 = \frac{a_+ q_+ - a_- q_-}{a_+ q_+ + a_- q_-} \frac{(u_+ - u_-)}{2\lambda}, \tag{8.8a}$$

$$\sigma^2 = 2DT - \frac{3}{4} \frac{(u_+ - u_-)^2}{\lambda^2} - \xi_0^2. \tag{8.8b}$$

Figure 3(*a*, *b*) compares the tilted-Gaussian approximation for c_+ with the exact solutions in the dead-zone situation

$$u_- = 0, \quad u_+ = \tfrac{3}{2}\bar{u} \quad (a_- = \tfrac{1}{3}, \quad a_+ = \tfrac{2}{3}). \tag{8.9}$$

There is no counterpart to the concentration spikes. However, for moderately large values of λt the tilted Gaussian is reasonably accurate, and does achieve its objective of yielding suitably skew concentration distributions.

For a uniform discharge $q_+ = q_- = \bar{q}$ at $x = 0, t = 0$ the exact solution for $\bar{c}$ has the continuous part $(u_- t < x < u_+ t)$

$$\bar{c} = \frac{\bar{q} 2 a_+ a_- \lambda}{u_+ - u_-} \left\{ I_0(r) + \lambda \frac{(a_+(x - u_- t) + a_-(u_+ t - x))}{(u_+ - u_-) r} I_1(r) \right\} \times \exp\left\{ -\lambda \frac{(a_-(x - u_- t) + a_+(u_+ t - x))}{u_+ - u_-} \right\}, \tag{8.10a}$$

with

$$r^2 = 4\lambda^2 a_+ a_- \frac{(x - u_- t)(u_+ t - x)}{(u_+ - u_-)^2}, \tag{8.10b}$$

plus the pair of decaying-delta-function spikes

$$\bar{c} = a_- \bar{q} \delta(x - u_- t) \exp(-a_+ \lambda t), \tag{8.10c}$$

$$\bar{c} = a_+ \bar{q} \delta(x - u_+ t) \exp(-a_- \lambda t). \tag{8.10d}$$

The Gaussian approximation (7.5) or (7.8) for the component concentrations c_+ and c_- leads to a composite formula

$$\bar{c} = \frac{\bar{q}}{(2\pi\langle\sigma^2\rangle)^{\frac{1}{2}}} \left\{ a_+ \exp\left[-\frac{1}{2\langle\sigma^2\rangle} \left(x - \bar{u}t - \frac{a_+(u_+ - u_-)}{\lambda} \right)^2 \right] + a_- \exp\left[-\frac{1}{2\langle\sigma^2\rangle} \left(x - \bar{u}t + a_- \frac{(u_+ - u_-)}{\lambda} \right)^2 \right] \right\} \tag{8.11a}$$

with

$$\langle\sigma^2\rangle = \frac{(u_+ - u_-)^2}{\lambda^2} \left\{ 2a_+ a_- \lambda t - (a_+ - a_-) \frac{\lambda(x - \bar{u}t)}{u_+ - u_-} - \tfrac{3}{4} - (a_+ - a_-)^2 \right\}. \tag{8.11b}$$

Alternatively, the direct Gaussian approximation (7.12) for $\bar{c}$ is

$$\bar{c} = \frac{\bar{q}}{(2\pi\Sigma^2)^{\frac{1}{2}}} \exp\left[-\frac{1}{2\Sigma^2} \left(x - \bar{u}t - (a_+ - a_-) \frac{(u_+ - u_-)}{\lambda} \right)^2 \right], \tag{8.12a}$$

with

$$\Sigma^2 = \frac{(u_+ - u_-)^2}{\lambda^2} \left\{ 2a_+ a_- \lambda t - (a_+ - a_-) \lambda \frac{(x - \bar{u}t)}{u_+ - u_-} - \tfrac{1}{2} - (a_+ - a_-)^2 \right\}. \tag{8.12b}$$

Figure 4 compares these double and single tilted-Gaussian distributions with the exact solution in the dead-zone situation (8.9). The approximate distributions are

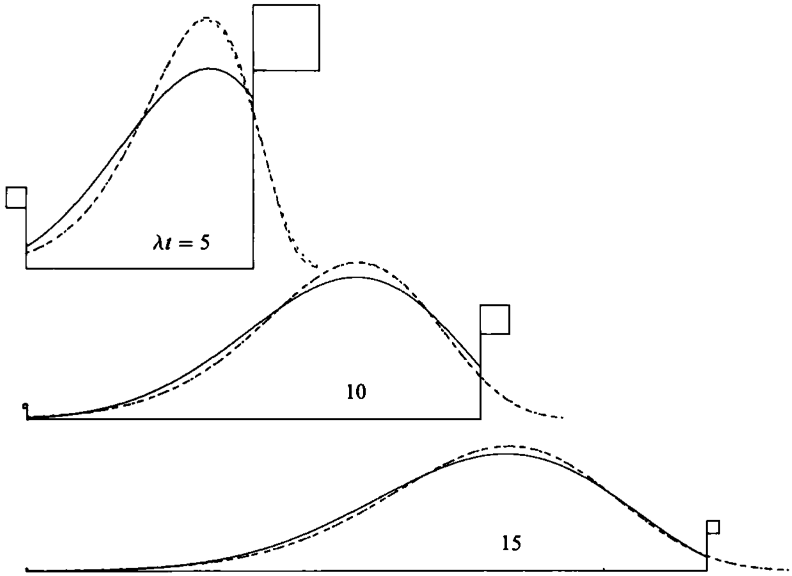

FIGURE 4. Comparison between the exact (——), double tilted Gaussian (– – – –), and single tilted Gaussian (· · · ·) at times $\lambda t = 5, 10, 15$ for the cross-sectionally averaged concentration $\bar{c}$ with a uniform discharge in a two-layer flow. The area under the delta-function spikes is indicated by the area of the flags.

virtually indistinguishable from each other. For modest values of λt the skewness is well reproduced. It is the negative kurtosis (flat centre and the absence of tails) that gives the dominant error.

9. Plane Poiseuille flow

To discriminate between the Gaussian approximations (7.5) and (7.8) we need an example for which the excess variance function $R(y, z)$ is non-zero, and for which exact results are available at suitably large times. This second constraint leads us to consider plane Poiseuille flow, which has been investigated numerically by Jayaraj & Subramanian (1978).

The velocity profile is parabolic:

$$u = \tfrac{3}{2}\bar{u}\left[1-\left(\frac{y}{d}\right)^2\right] \quad (-d < y < d) \tag{9.1}$$

and the centroid displacement function is a quartic:

$$g(y) = \frac{\bar{u}d^2}{\kappa}\left\{\frac{17}{264}-\frac{1}{4}\left(\frac{y}{d}\right)^2+\frac{1}{8}\left(\frac{y}{d}\right)^4\right\}. \tag{9.2}$$

The integrals $\overline{ug}, \overline{g^2}, \bar{g}$ can all be evaluated explicitly:

$$D = \frac{2}{105}\frac{\bar{u}^2d^2}{\kappa}, \quad \overline{g^2} = \frac{163}{73\,920}\frac{\bar{u}^2d^4}{\kappa^2}, \quad \alpha = -\frac{7}{22\bar{u}}. \tag{9.3}$$

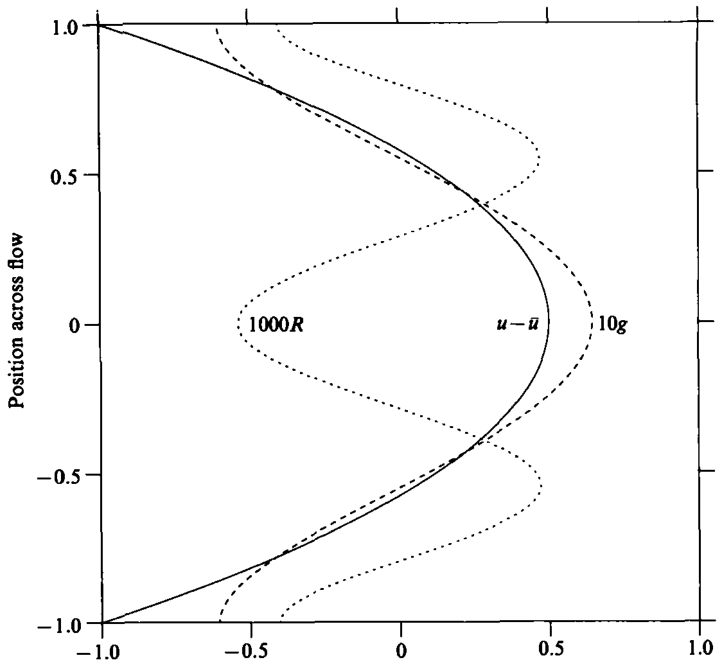

FIGURE 5. The relative shapes across the flow of the non-dimensional functions $(u/\bar{u})-1$ log $\kappa/d^2\bar{u}$, $1000R\kappa^2/d^4\bar{u}^2$ for plane Poiseuille flow.

Solving (7.4*a–c*) we find that the excess variance function is a polynomial of degree 8:

$$R(y)=\frac{\bar{u}^2d^4}{\kappa^2}\left\{-\frac{299}{554400}+\frac{37}{4620}\left(\frac{y}{d}\right)^2-\frac{53}{2640}\left(\frac{y}{d}\right)^4+\frac{1}{60}\left(\frac{y}{d}\right)^6-\frac{1}{224}\left(\frac{y}{d}\right)^8\right\}.$$

Figure 5 compares the shapes of the velocity profile $u-\bar{u}$, the centroid displacement function $g(y)$, and the variance function $R(y)$. The dimensional factors $\bar{u},\kappa,d$ have been ignored, g has been scaled up by a factor 10, and R has been scaled up by a factor of 1000. General features that are exhibited by this special case are the similarity between the $(u-\bar{u})$- and g-profiles, and the comparative smallness of R compared to g^2. We note that $R(y)$ is negative both at the centre and near the sides. Thus, the shear dispersion process is less efficient, with reduced longitudinal spreading, where the velocity shear is small and also close to a boundary. Hence, the approximation (7.8), which neglects the $2R(y)$ contribution to σ^2, will slightly underestimate the concentrations in the fastest and slowest moving parts of the contaminant cloud, with slight overestimates in the middle of the cloud.

Figure 6 compares the concentration contours given by the tilted Gaussian (7.5) and by the simplified formula (7.8) (neglecting $R(y)$) at the time $t=0.4d^2/\kappa$. Following Jayaraj & Subramanian (1978, figure 4), the initial discharge is assumed to have been uniform across the flow, with a longitudinal spread of $0.04\bar{u}d^2/\kappa$. Also, there is a direct longitudinal diffusion contribution of $0.004\bar{u}^2d^2/\kappa$ to D. These are accounted for by appropriate increments to σ^2 and to $\langle\sigma^2\rangle$. The dominant feature of the concentration contours is their centroid-following character. Although there are not major quantitative differences, there is the qualitative difference of the

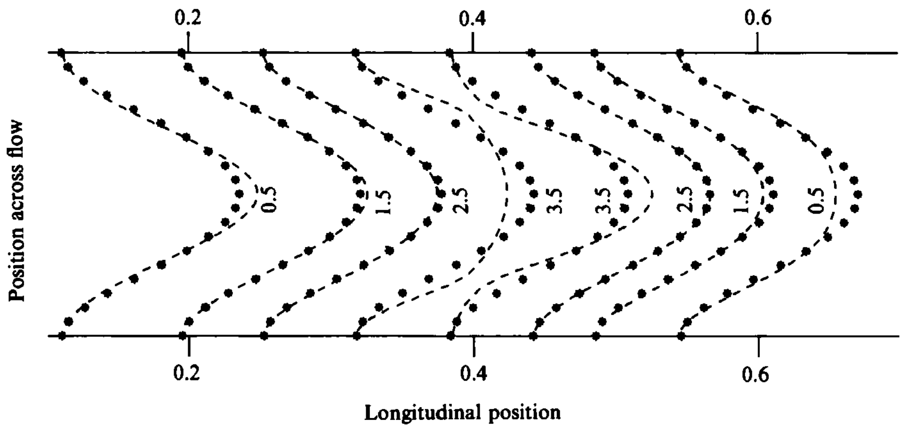

FIGURE 6. Concentration contours for plane Poiseuille flow at time $0.4d^2/\kappa$ after discharge as predicted by the tilted Gaussian including $R(y)$ (----), and the tilted Gaussian neglecting $R(y)$ (* * *).

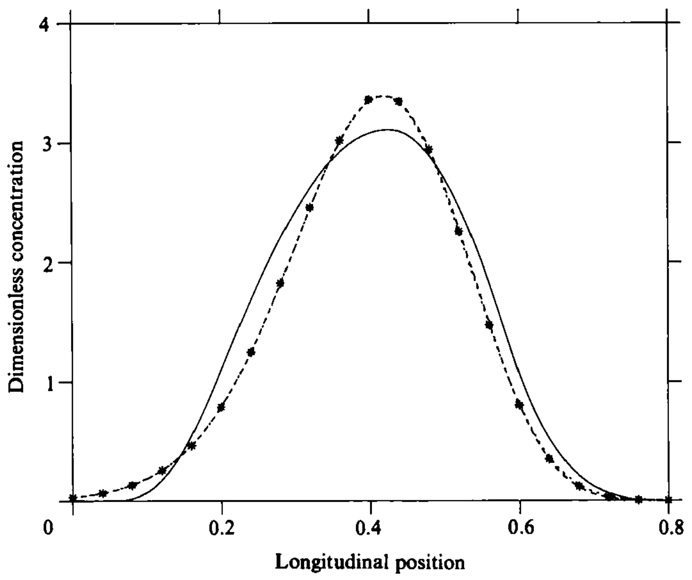

FIGURE 7. Comparison between Jayaraj & Subramanian's (1978) exact result for $\bar{c}$ (——), the average of the tilted Gaussian including $R(y)$ (----), the average of the tilted Gaussian neglecting $R(y)$ (* * *), and the direct formula for $\bar{c}$ (····) at a time $0.4d^2/\kappa$ after discharge in plane Poiseuille flow.

high-concentration patches at the centre and side of the flow for the full Gaussian (7.5).

Jayaraj & Subramanian (1978, figure 4) present numerical results for the cross-sectionally averaged concentration $\bar{c}$. Figure 7 shows the exact results together with the cross-sectional averages of (7.5) and (7.8) and the direct tilted Gaussian formula (7.12) for $\bar{c}$. Again, the various tilted Gaussian approximations are virtually indistinguishable, showing the rapid convergence of the series (7.7) and (7.11).

An important restriction upon the present analysis is that it is only applicable at large times after discharge, when the contaminant has become well mixed across the flow. (Otherwise the predicted variance Σ^2 can be negative!) Subject to this restriction, the results given by the tilted Gaussian formulae are of comparable accuracy with those given by other more complicated models (see Smith 1981, figure 7). To do better, and to reproduce the flatness of the profile, would require an extension of the calculations to evaluate the fourth moment and to go beyond the Gaussian approximation.

I wish to thank the Royal Society for financial support.

Appendix. Field-flow fractionation

In the context of the work of Jayaraj & Subramanian (1978), the results shown in figure 7 above are anomalous in the very weak skewness. To give a more convincing demonstration of the usefulness of the tilted-Gaussian approximation, this Appendix investigates the effect of a transverse drift upon contaminant dispersion.

In the original (x, y, t)-coordinates the advection–diffusion equation takes the form

$$\partial_t c + u\,\partial_x c + \partial_y(vc) - \partial_y(\kappa\,\partial_y c) = q, \tag{A 1a}$$

with

$$vc - \kappa\,\partial_y c = 0 \quad \text{on } y = y_-, y_+. \tag{A 1b}$$

The transverse drift v is associated with a transverse force field (centrifugal, electrical, gravitational, magnetic or thermal) and can be a function of chemical species. When there is a longitudinal flow this drift away from regions of high (or low) velocity can lead to longitudinal separation of the component species in a mixture. The combined roles of the force field and of the longitudinal flow have led to the name 'field-flow fractionation'.

The equilibrium profile of concentration across the flow is given by

$$\gamma(y) = \exp\left(\int_{y_0}^{y} \frac{v}{\kappa}\,\mathrm{d}y'\right), \quad \overline{\gamma} = 1, \tag{A 2}$$

where the reference level y_0 is chosen so that the cross-sectional average value $\overline{\gamma} = 1$ is correctly reproduced. If we write

$$c = f(x, y, t)\,\gamma(y), \tag{A 3}$$

then the equation satisfied by f can be written

$$\gamma\,\partial_t f + \gamma u\,\partial_x f - \partial_y(\gamma\kappa\,\partial_y f) = q, \tag{A 4a}$$

with

$$\kappa\,\partial_y f = 0 \quad \text{on } y = y_-, y_+. \tag{A 4b}$$

Thus, instead of the transverse drift term, there is a profusion of γ-weighting factors in the advection–diffusion equation.

It is now merely a matter of including the appropriate γ-factors in the results of the above paper. In particular, a generalization of the simplest of the tilted-Gaussian formulae (7.12) for a sudden discharge at $x = 0, t = 0$ is

$$\overline{c} = \frac{\overline{q}}{(2\pi\Sigma^2)^{\frac{1}{2}}} \exp\left(-\frac{(x - u_{00}t - x_0 + 2\alpha D)^2}{2\Sigma^2}\right), \tag{A 5a}$$

where
$$u_{00} = \overline{\gamma u}, \quad (A\ 5b)$$
$$x_0 = \frac{\overline{g_0 q}}{\overline{q}}, \quad (A\ 5c)$$
$$D = \overline{\gamma(u-u_{00})g_0}, \quad (A\ 5d)$$
$$\alpha = \frac{\overline{\gamma(u-u_{00})g_0^2}}{2D^2}, \quad (A\ 5e)$$
$$\Sigma^2 = 2Dt+2\alpha D(x-u_{00}t)-3\overline{\gamma g_0^2}+\frac{\overline{g_0^2 q}}{\overline{q}}-\left(\frac{\overline{g_0 q}}{\overline{q}}\right)^2-4\alpha^2 D^2. \quad (A\ 5f)$$

The centroid displacement function $g_0(y)$ is defined by the cross-stream equations
$$\frac{d}{dy}\left(\gamma\kappa\frac{d}{dy}g_0\right) = \gamma(u_{00}-u), \quad (A\ 6a)$$
$$\gamma\kappa\frac{d}{dy}g_0 = 0 \quad \text{on } y = y_-, y_+, \quad (A\ 6b)$$
$$\overline{\gamma g_0} = 0. \quad (A\ 6c)$$

By construction the approximation (A 5*a*) correctly reproduces the asymptotic area, centroid and growth rates of the second and third moments. There can be a small error $(2\overline{Rq}/\overline{q})$ in the variance if the discharge shape $q(y)$ does not correspond to the equilibrium profile $\gamma(y)$.

For plane Poiseuille flow with constant v and κ the equilibrium profile of concentration across the flow is exponential:
$$\gamma = \frac{P}{\sinh P}\exp\left(\frac{Py}{d}\right), \quad (A\ 7a)$$
where
$$P = \frac{vd}{\kappa}. \quad (A\ 7b)$$

The weighted-average advection velocity u_{00} is given by the formula
$$\overline{u}\left(\frac{3\coth P}{P}-\frac{3}{P^2}\right) \quad (A\ 8)$$
and the centroid displacement function has the explicit solution
$$\frac{\kappa g_0}{d^2\overline{u}} = \frac{6}{P^4}+\frac{9}{2P^2}-\left(\frac{3}{P^3}-\frac{1}{P}\right)\coth P-\frac{6}{P^2}\coth^2 P+\left(\frac{3}{P^2}\coth P-\frac{3}{2P}\right)Y$$
$$-\frac{3}{2P^2}Y^2+\frac{1}{2P}Y^3+\frac{3}{P^3\sinh P}e^{-PY}. \quad (A\ 9)$$

The many integrals involving g_0 can most easily be evaluated by numerical quadrature, although Krishnamurthy & Subramanian (1977, equation (A 31)) do state the explicit formula for the shear dispersion coefficient:
$$\frac{\kappa}{\overline{u}^2 d^2}D = \frac{9}{P^4\sinh P}\left[\frac{2P^2}{3\sinh P}-\frac{10\cosh P}{P}+\frac{14\sinh P}{P^2}+\frac{2}{\sinh P}\right.$$
$$\left.-\frac{2P\cosh P}{\sinh^2 P}-\frac{4\cosh^2 P}{\sinh P}+6\sinh P\right]. \quad (A\ 10)$$

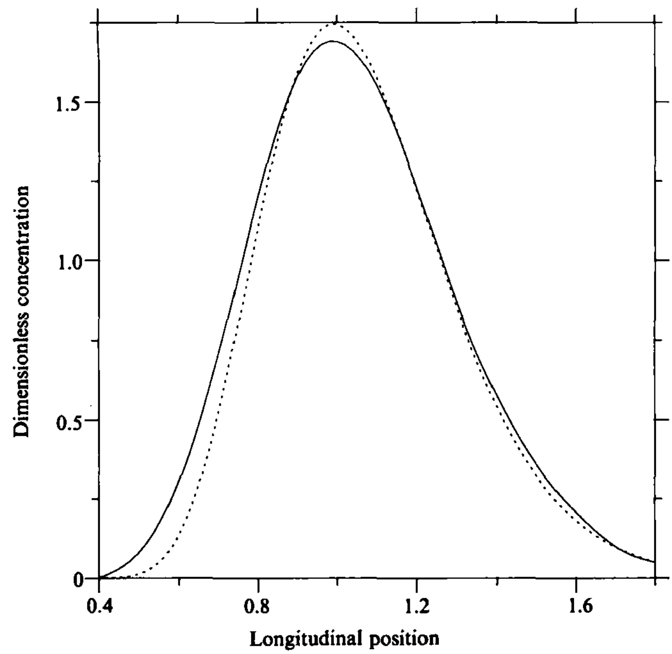

FIGURE 8. Comparison between Jayaraj & Subramanian's (1978) exact results for $\bar{c}$ (——), and the tilted Gaussian formula for $\bar{c}$ (····), at a time $2d^2/\kappa$ after discharge in plane Poiseuille flow with a transverse drift $vd/\kappa = 5$.

Jayaraj & Subramanian (1978, figure 13) give the $\bar{c}$-distribution for field flow fractionation with $P = 5$ at a time $t = 2d^2/\kappa$ after a uniform discharge. The terms needed for the evaluation of the tilted-Gaussian approximation (A 5*a*) are

$$\left.\begin{aligned} &\frac{u_{00}}{\bar{u}} = 0.48, \quad \frac{x_0 \kappa}{\bar{u}d^2} = 0.11, \quad \frac{D\kappa}{\bar{u}^2 d^2} = 0.00807, \\ &\overline{\gamma(u-u_{00})\, g_0^2}\,\frac{\kappa^2}{\bar{u}^3 d^4} = 0.000426, \quad \overline{\gamma g_0^2}\,\frac{\kappa^2}{\bar{u}^2 d^4} = 0.000626, \\ &\overline{g_0^2}\,\frac{\kappa^2}{\bar{u}^2 d^4} = 0.0182. \end{aligned}\right\} \qquad (\text{A } 11a\text{–}f)$$

As before, the effects of longitudinal diffusion and of the initial discharge size can be allowed for by an appropriate increment to Σ^2. Figure 8 shows the efficiency of the tilted Gaussian. The substantially later time than that for figure 7 explains the improved accuracy. More importantly, the marked skewness is accurately reproduced.

REFERENCES

ABRAMOWITZ, M. & STEGUN, I. A. 1965 *Handbook of Mathematical Functions*. Dover.

ARIS, R. 1956 On the dispersion of a solute in a fluid flowing through a tube. *Proc. R. Soc. Lond.* A **235**, 67–77.

BARTON, N. G. 1983 The method of moments for solute dispersion. *J. Fluid Mech.* **136**, 243–267.

CHATWIN, P. C. 1970 The approach to normality of the concentration distribution of a solute in solvent flowing along a straight pipe. *J. Fluid Mech.* **43**, 321–352.

CHATWIN, P. C. 1980 Presentation of longitudinal dispersion data. *J. Hydraul. Div. ASCE* **106**, 71–83.

CHICKWENDU, S. C. & OJIAKOR, G. U. 1985 Slow-zone model for longitudinal dispersion in two-dimensional shear flows. *J. Fluid Mech.* **152**, 15–38.

GILL, W. N. & SANKARASUBRAMANIAN, R. 1970 Exact analysis of unsteady convective diffusion. *Proc. R. Soc. Lond.* A **327**, 191–208.

KRISHNAMURTHY, S. & SUBRAMANIAN, R. S. 1977 Exact analysis of field-flow fractionation. *Sep. Sci. Tech.* **12**, 347–379.

JAYARAJ, K. & SUBRAMANIAN, R. S. 1978 On relaxation phenomena in field-flow fractionation. *Sep. Sci. Tech.* **13**, 791–817.

NADIM, A., PAGITSAS, M. & BRENNER, H. 1986 Higher-order moments in macrotransport processes. *J. Chem. Phys.* **85**, 5238–5245.

SMITH, R. 1981 A delay-diffusion description for contaminant dispersion *J. Fluid Mech.* **105**, 469–486.

SMITH, R. 1984 Temporal moments at large distances downstream of contaminant releases in rivers. *J. Fluid Mech.* **140**, 153–174.

TAYLOR, G. I. 1953 Dispersion of soluble matter in solvent flowing slowly through a tube. *Proc. R. Soc. Lond.* A **219**, 186–203.

THACKER, W. C. 1976 A solvable model of shear dispersion. *J. Phys. Oceanogr.* **6**, 66–75.

TSAI, Y. H. & HOLLEY, E. R. 1978 Temporal moments for longitudinal dispersion. *J. Hydraul. Div. ASCE* **104**, 1617–1634.

TSAI, Y. H. & HOLLEY, E. R. 1980 Temporal moments for longitudinal dispersion. *J. Hydraul. Div. ASCE* **106**, 2063–2066.